Passive vibration control of offshore wind turbines using structure-immittance approach

Yi-Yuan Li [1], **Sara Ying Zhang** [1], **Jason Zheng Jiang** [1], **Simon Neild** [1], **Ian Ward** [2]
[1] University of Bristol, Department of Mechanical Engineering,
Senate House, Tyndall Avenue, Bristol, BS8 1TH, UK.
yiyuan.li@bristol.ac.uk; **yz13229@bristol.ac.uk**; **z.jiang@bristol.ac.uk**; **simon.neild@bristol.ac.uk**

[2] SNC-Lavalin Atkins,
Epsom, Surrey, UK.
Ian.Ward@atkinsglobal.com

Abstract
Offshore wind turbines are growing in popularity due to the steady, high speed and environment friendly offshore wind resources. However, the wind and wave excitations can result in excessive vibration and hence destroying the structural integrity. To avoid this, the inerter-based vibration absorber, which is a reaction mass connected to the system with the combinations of springs, dampers and inerters, is employed in this study to suppress the vibration. Both monopile and spar-buoy offshore wind turbines are investigated in this paper by establishing limited degree-of-freedom models based on FAST. The structure-immittance approach is used to obtain the optimal absorber configurations with corresponding element values, by minimising the standard deviation of the tower top displacement. It will be shown that compared with the traditional tuned mass damper, the performance of the inerter-based absorber is superior. Moreover, with the same performance as the tuned mass damper, the mass of the inerter-based absorber can be significantly reduced.

1 Introduction

Offshore wind turbines (OWTs) are growing in popularity due to the steady, high speed and environment friendly offshore wind resources. However, the combined multiple hazards such as wind and wave excitations can result in excessive vibration and fatigue load, hence destroying the structural integrity, shortening the service life and increasing the energy production cost of the turbines. In order to prolong its lifespan, passive structural control strategy, which is widely used due to its simplicity and zero power input, is employed in this paper for the vibration suppression of the OWTs.

The most commonly used passive structural control device is the tuned mass damper (TMD). Murtagh et al. [1] studied the vibration mitigation of a blade coupling wind turbine model by using a TMD under the along-wind force; Lackner et al. [2] included a TMD into the FAST code [3], a fully coupled aero-hydro-servo-elastic code developed by National Renewable Energy Laboratory (NREL) to simulate the loads and performance of OWTs; Later Stewart et al. [4] optimised the parameter values of a TMD based on the limited degree-of-freedom (DOF) models; Stewart et al. [5] also investigated the effects of misalignment for the OWTs with a TMD in the nacelle; Specifically, Si et al. [6] investigated the vibration suppression of a spar-type floating OWT by employing a TMD in the platform. Even though the performance of the TMD will be improved as the mass of the TMD increasing, due to the space and weight limitation, performance of the TMD is limited. In order to enhance the vibration suppression capability of the TMD, a passive mechanical

element, the inerter, is employed in the present study.

The inerter was first introduced by Smith [7]. It is a two-terminal device with the property that the force generated is proportional to the relative acceleration across its two terminals. With inerter, the force-current analogy [8] between mechanical and electrical systems can be fully achieved, with mechanical elements springs, dampers and inerters corresponding to the electrical elements inductors, resistors and capacitors, respectively. For passive electrical networks, using the Bott-Duffin theorem [9], it has been shown that any positive-real functions can be realised as the driving-point immittance of a network consisting only of resistors, capacitors and inductors. Hence, mechanical networks consisting of dampers, inerters and springs can also synthesise all positive-real functions characterising force-velocity properties. In general, two approaches are applied to identify beneficial passive vibration absorber, the structure-based approach and the immittance-based approach. For the structure-based approach, network layouts, such as the TID [10] and the TMDI [11], are first proposed. Parameter values for the constituent elements are then selected based on performance criteria. With this approach, the complexity and topology of the absorber is pre-determined. However, only one network layout can be considered at a time even though there are large number of possible layouts, which inevitably limits the achievable performance of the proposed absorber. On the other hand, with the immittance-based approach, such as the application proposed by Wang et al. [12] and Li et al. [13], a positive-real immittance function which is capable of providing the optimum performance of the system is first obtained. Then, the corresponding network layout and element values can be identified using network synthesis theory. However, without pre-restricted complexity and topology of the network, undesirable networks with very complicated layouts may occur. To overcome the disadvantages of structure-based and immittance-based approaches, a novel structure-immittance approach was proposed by Zhang et al. [14] for passive vibration absorber identification. With this approach, a new class of structural immittance functions can be obtained, which can cover a full set of network layouts with explicit information of all topology possibilities; meanwhile, the number of each element type can be pre-determined, and the element values can be fixed or constrained.

In this paper, the NREL 5MW offshore wind turbine [15] is considered. An inerter-based absorber (IBA) is used to investigate the vibration suppression for both a fixed-bottom monopile and a floating spar-buoy platform. The structure-immittance method is employed to obtain the optimum absorber, which is a reaction mass connected to the nacelle at a single point using a combination of one inerter, one damper and two springs. This paper is constructed as follows: In Section 2, the structure-immittance method for one inerter, one damper and two springs case is briefly summarised; In Section 3, the limited DOF Matlab models of monopile and spar-buoy are established and the structure parameters are identified; In Section 4, the IBAs' layouts and corresponding parameter values are obtained for monopile and spar-buoy, respectively. The potential of mass reduction is also investigated in this section. Finally, conclusions are drawn in Section 5.

2 Structure-immittance method

By utilising the force-current analogy, the structure-immittance method can be applied both on mechanical and electrical networks. The transfer function of the mechanical network is defined as

$$Y(s) = \frac{F(s)}{V(s)} \tag{1}$$

where $F(s)$ and $V(s)$ are the force and relative velocity across the two terminals in Laplace domain, respectively. s is the complex frequency parameter of the Laplace transform. Mapping it to electrical system, the transfer function corresponds to the admittance of electrical networks, which is

$$Y(s) = \frac{I(s)}{U(s)} \tag{2}$$

where $I(s)$ and $U(s)$ are the current and voltage across the two terminals in Laplace domain, respectively. One-port (two-terminal) mechanical networks are taken into consideration to develop structure-immittance

method in this paper. The definition of structural-immittances, which include all the possible arrangements of a set number of elements, are given as the transfer functions from force to velocity. In this section, a mechanical system including one inerter, one damper and two springs as well as its structural-immittances are demonstrated.

For the case of one inerter, one damper and two springs, there are totally 18 absorber layouts. By using the structure-immittance method, two networks, termed Q_1 and Q_2, that contain all the 18 possible layouts, can be obtained. There are totally 4 steps needed to obtain the final networks Q_1 and Q_2 [14], for compliance these are summarised here. It should be noted that at most two springs are present for the networks obtained in each step.

Step 1: Two generic sub-networks M_1 and M_2 are constructed as shown in step 1 of Figure 1 . One is an inerter based sub-network and the other is a damper-based sub-network.

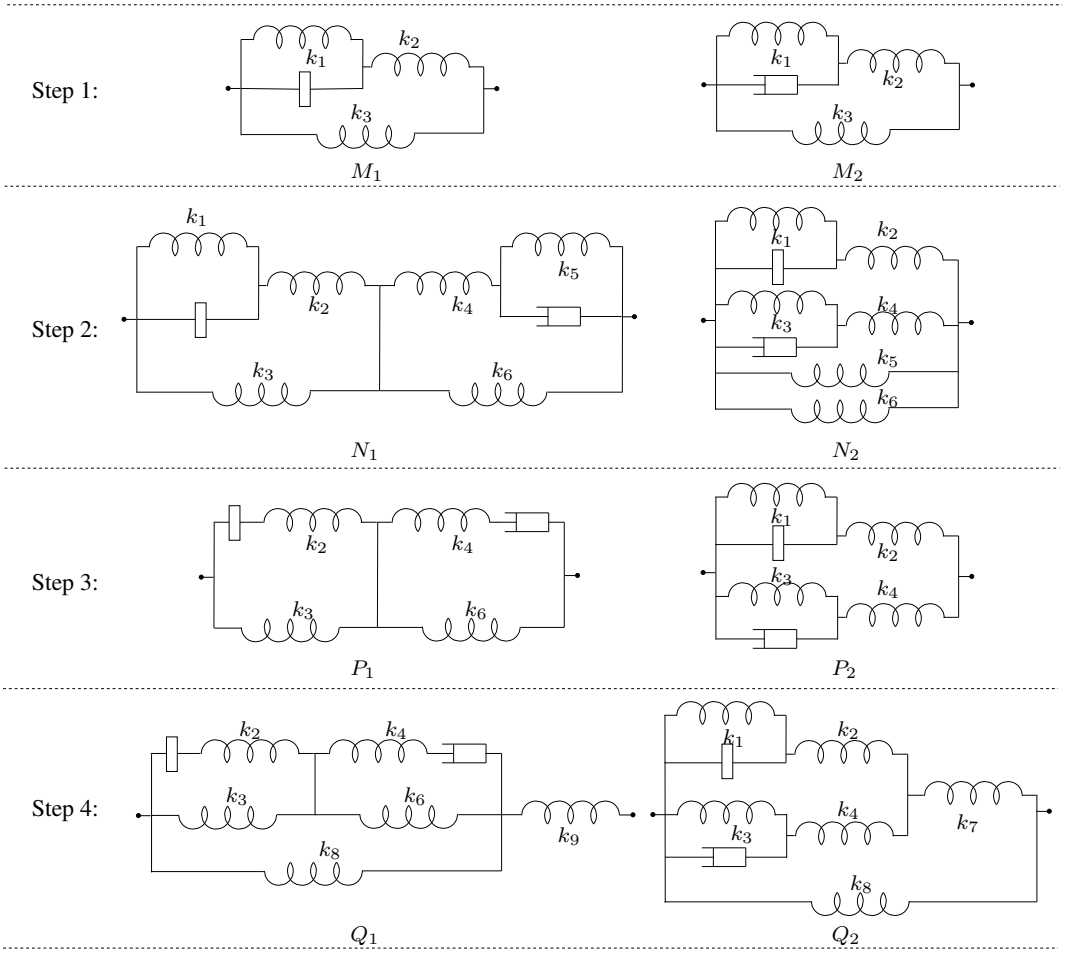

Figure 1: The networks obtained for 1 damper, 1 inerter and 2 springs

Step 2: Two sub-networks M_1 and M_2 are connected to each other both in parallel and in series to form two new networks N_1 and N_2, as shown in step 2 of Figure 1 .

Step 3: Since in networks N_1 and N_2, some of the springs are redundant and can produce the same effect on the network, redundancy of the springs in networks N_1 and N_2 need to be checked with springs removed if possible. For example, for k_1 in network N_1, the layout with k_1 and k_2 present can be realised by k_3 and k_4; the layout with k_1 and k_3 present can be realised by k_3 alone; the layout with k_1 and k_4 present is equivalent to that with k_3 and k_4; the layout with k_1 and k_5 present can be realised by k_3 and k_6; the layout with k_1 and k_6 present equals that with k_3 and k_6. Therefore, k_1 is redundant and can be removed. All of the springs in N_1 and N_2 should be checked one by one to guarantee that there is no redundancy left in the networks. As a result, two simplified networks P_1 and P_2 can be obtained, as shown in step 3 of Figure 1 .

Step 4: Springs are now added to the network to form the final networks. The adding rule is: a spring is first added in series and the redundancy is checked for this added spring. Then, another spring is added in parallel and the redundancy is checked. This process is repeated until any further addition of a spring in series or in parallel is redundant. Thus, the final networks can be constructed. Follow the adding rule, final networks, Q_1 and Q_2, are obtained, see step 4 of Figure 1 .

The structural-immittances of networks Q_1 and Q_2 are:

$$Y_i(s) = \frac{n_i(s)}{m_i(s)} \quad (i = 1, 2), \tag{3}$$

where

$$\begin{aligned}
n_1(s) =& bc(k_3/k_2 + k_8/k_2 + k_6/k_4 + k_8/k_4 + 1)s^3 + b(k_6 + k_8)s^2 + \\
& c(k_3 + k_8)s + k_3k_6 + k_3k_8 + k_6k_8, \\
m_1(s) =& s\big[bc(1/k_2 + 1/k_4 + 1/k_9)s^3 + b(k_3/k_2 + k_6/k_2 + k_6/k_9 + k_8/k_9 + 1)s^2 + \\
& c(k_3/k_4 + k_3/k_9 + k_6/k_4 + k_8/k_9 + 1)s + k_3 + k_6\big], \\
n_2(s) =& bc(1/k_2 + 1/k_4)s^3 + b(k_3/k_2 + k_3/k_4 + k_8/k_2 + k_8/k_7 + 1)s^2 + \\
& c(k_1/k_2 + k_8/k_4 + k_1/k_4 + k_8/k_7 + 1)s + k_1 + k_3 + k_8, \\
m_2(s) =& s\big[bc(1/(k_2k_4) + 1/(k_2k_7) + 1/(k_4k_7))s^3 + b(1/k_2 + 1/k_7)s^2 + \\
& c(1/k_4 + 1/k_7)s + k_1/k_2 + k_1/k_7 + k_3/k_4 + k_3/k_7 + 1\big].
\end{aligned} \tag{4}$$

$Y_1(s)$ and $Y_2(s)$ include all the possibilities of one inerter, one damper and two springs combinations. For $Y_1(s)$, only two of $1/k_2$, k_3, $1/k_4$, k_6, k_8 and $1/k_9$ are positive and all the others are equal to zero. For $Y_2(s)$, only two of k_1, $1/k_2$, k_3, $1/k_4$, $1/k_7$ and k_8 are positive and all the others are equal to zero. These transfer functions can be used, along with the constraints listed here to find the optimal one inerter, one damper and two springs configuration for a given system and objective function.

3 Limited DOF offshore wind turbine models

The ideal way to identify the IBA configurations and their corresponding parameters would be to carry out the optimisation within FAST. However, the inerter and the structure-immittance approach have not been included in FAST so far. Besides, FAST is expensive in terms of the computations needed since the simulation time in FAST for a 60 s simulating is around 60 s, and to find the optimum values, thousands of function calls might be needed. As a feasibility study, following [4], a limited DOF linear Matlab model for each type of OWT is established in this section.

3.1 Monopile

Considering the monopile, the tower fore-aft bending mode is responsible for most of the fatigue loading. Hence two DOFs are considered here: the tower fore-aft bending DOF and the IBA's mass DOF. The model is shown in Figure 2 (a). Applying the small angle approximation, equations of motion of the system are given as:

$$\begin{cases} m\ddot{x}_r = & mg\theta_t - Y\dot{x}_r - mR\ddot{\theta}_t \\ I_t\ddot{\theta}_t = & m_tgR_t\theta_t + RY\dot{x}_r - k_t\theta_t - c_t\dot{\theta}_t + mgx_r \end{cases} \tag{5}$$

where m_t is the turbine's total mass and m is the absorber's mass. The angle that the tower has deflected from vertical is denoted by θ_t. Nacelle of the OWT is considered as a reference frame and the displacement of the

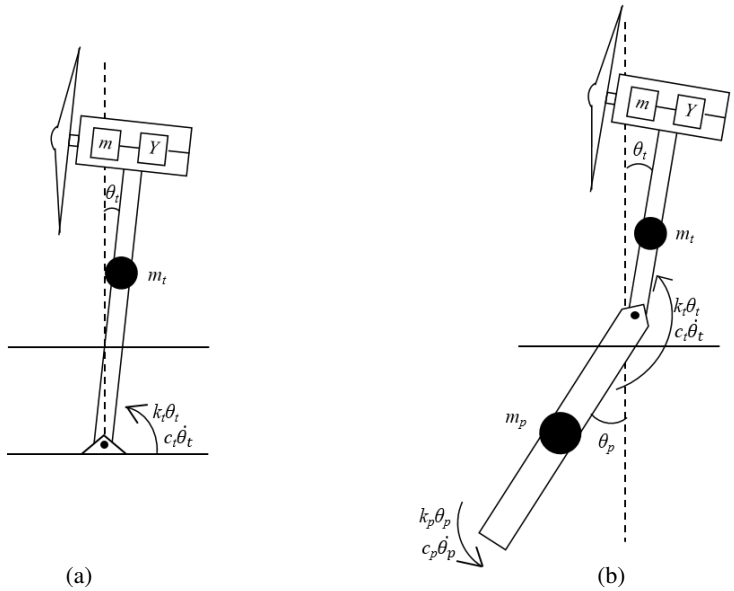

Figure 2: Limited DOF offshore wind turbine model inspired by [4]: (a) monopile; (b) spar-buoy.

absorber is relative to the nacelle, which is denoted as x_r. So the term $mR\ddot{\theta}_t$ exists due to the non-inertial reference frame. R and R_t are the distances from the tower hinge to the absorber and the centre of the turbine total mass, respectively. k_t and c_t are the rotary stiffness and rotary damping constants at the tower base. Y is the representation of the admittance function of absorbers consisting of inerters, dampers and springs. The absorber's mass m is taken to be equal to 20,000 kg for consistence with [4] and it is approximately 2% of the turbine's total mass m_t.

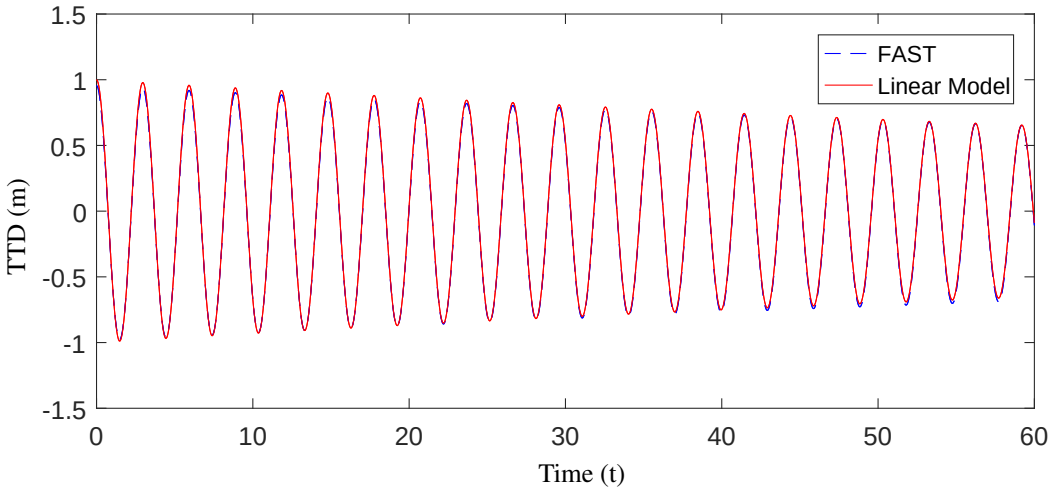

Figure 3: Response comparison of linear model and FAST for monopile

In order to use the linear model to obtain the optimal absorber's configuration, model parameters must be determined first. I_t, m_t, R_t and R can be obtained from [16, 17] and the FAST input files. The rotary stiffness k_t and the rotary damping constants c_t need to be determined by matching the linear model response to FAST output with the same input conditions. In this paper, a step input of the tower top displacement (TTD) equal to 1 m is used, which is the amount of tower bending in meters measured at the top of the tower. The response of the linear model is fitted into the FAST output in Matlab where the plot of the fit of the TTD for the monopile model is shown in Figure 3 . The monopile TTD starts at 1 m and oscillates at a frequency of approximately 0.337 Hz. It can be observed from Figure 3 that the responses of the limited DOF monopile Matlab model and the FAST output are very close to each other. The resulting rotary stiffness and rotary

damping values are $k_t = 2.52 \times 10^{10}$ kN·m/rad and $c_t = 7.75 \times 10^7$ kN·m·s/rad, respectively. The obtained parameters are listed in Table 1 .

Properties	Values
Hub mass	56780 kg
Nacelle mass	240000 kg
Rotor mass	110000 kg
Tower and monopile mass	522617 kg
Turbine total Mass m_t	929397 kg
absorber's mass m	20000 kg
Tower inertia I_t	5.43×10^9 kg·m^2
Turbine's height R	107.6 m
Mass centre to the bottom R_t	76.4 m
Rotary stiffness constant k_t	2.52×10^{10} kN·m/rad
Rotary damping constant c_t	7.75×10^7 kN·m·s/rad

Table 1: Monopile model parameters

3.2 Spar-buoy

For the spar-buoy, the tower fore-aft bending mode and the platform pitch angle mode are responsible for most of the fatigue loading. Therefore, there are three DOFs that are of concern: the tower fore-aft bending DOF, the platform pitch DOF and the absorber's mass DOF. The model is shown in Figure 2 (b) . Similarly, applying the small angle approximation and considering the absorber in the non-inertial reference frame, the equations of motion of the system are given as:

$$\begin{cases} m\ddot{x}_r = mg\theta_t - Y\dot{x}_r - mR\ddot{\theta}_t \\ I_t\ddot{\theta}_t = m_t g R_t\theta_t + RY\dot{x}_r - k_t(\theta_t - \theta_p) - c_t(\dot{\theta}_t - \dot{\theta}_p) + mgx_r \\ I_p\ddot{\theta}_p = -m_p g R_p\theta_p + k_t(\theta_t - \theta_p) + c_t(\dot{\theta}_t - \dot{\theta}_p) - k_p\theta_p - c_p\dot{\theta}_p \end{cases} \tag{6}$$

where m_p is the mass of the platform; θ_p is the angle that the platform has bent from vertical; R_p is the distance from the tower hinge to the centre of the platform mass; k_p and c_p are the rotary stiffness and damping constants of spar-buoy platform, which are the summation of hydrostatic and mooring line effects and so on. All the other parameters have the same values as those used in the monopile linear model.

Again, the model parameters must be determined first. Similarly, m_t, I_t, m_p, R, R_t and R_p can be obtained from [18] and the FAST input files. The tower and platform rotary stiffness and damping constants k_t, c_t, k_p and c_p, respectively, will be identified by comparing the model to FAST outputs in Matlab. In addition, the platform inertia I_p needs to be identified, this is because inertial effect of the water must also be considered in I_p. The platform inertia shown in the FAST input file is the true platform inertia, whereas for the simplified model, since the platform is under the sea, this effect is significant. For the spar-buoy type OWT, a step input of the platform pitch angle equal to 5° is used to obtain the FAST monopile model output. Figure 4 (a) and (b) show the plot of the fit for the TTD and the platform pitch angle (PPA) for the spar-buoy model in Matlab. Since the TTD reflects the tower bending condition, TTD is relative to the platform coordinate system. This means if the platform is pitched while there is no bending of the tower, then the TTD is zero. The spar-buoy PPA starts at 5° with the frequency of approximately 0.019 Hz and the TTD starts at 1 m with the frequency of approximately 0.377 Hz. It can be observed from Figure 4 that the fit between the limited DOF spar-buoy model and the FAST output is reasonable. The inaccuracies in the model are because the spar-buoy damping constant c_p includes many sources of hydrodynamic damping, wave radiation and viscous damping. These terms are nonlinear, and so are only approximated in the linear damping constants used in the low order linear model. The resulting rotary stiffness and damping constants of tower and

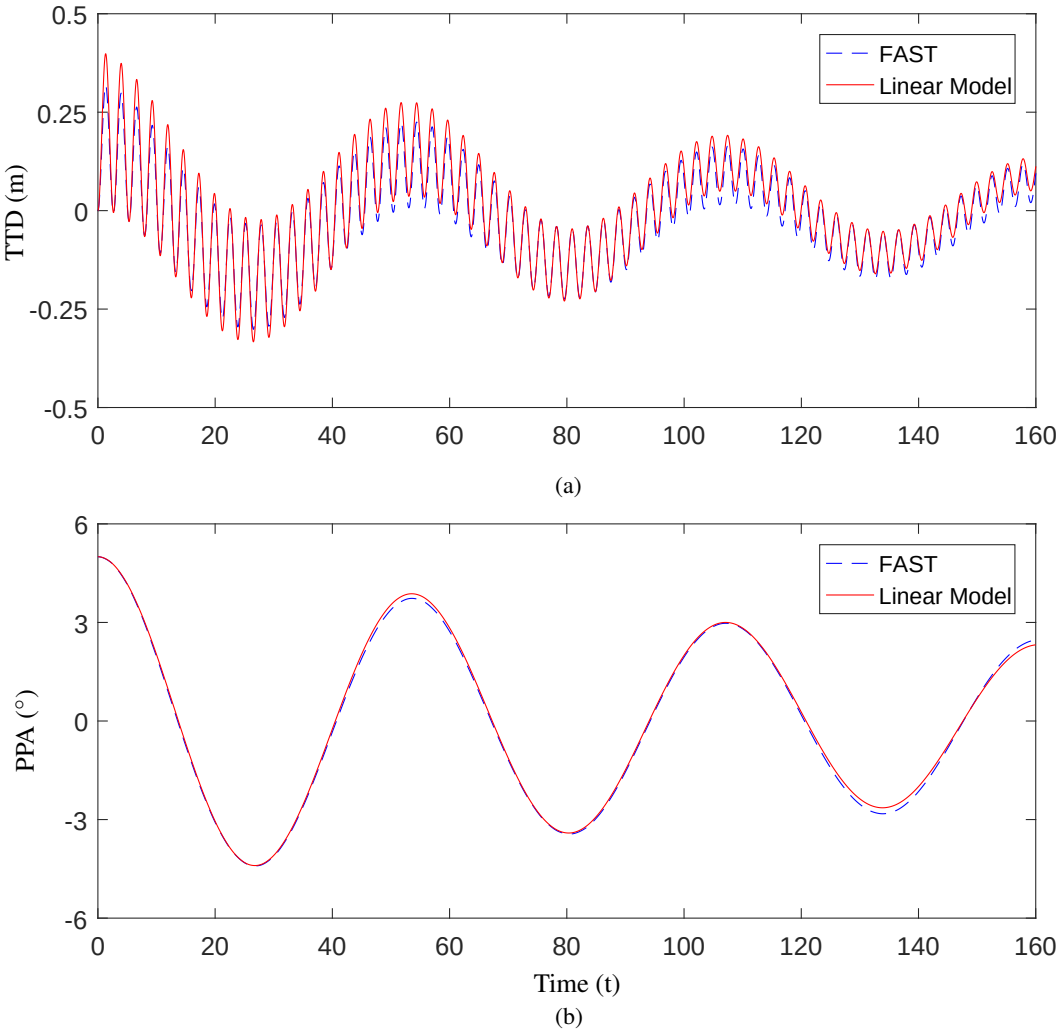

Figure 4: Response comparison of linear model and FAST for spar-buoy: (a) TTD; (b) PPA.

platform are $k_t = 1.56 \times 10^{10}$ kN·m/rad, $c_t = 5.32 \times 10^7$ kN·m·s/rad, $k_p = 6.00 \times 10^7$ kN·m/rad and $c_p = 5.42 \times 10^9$ kN·m·s/rad, respectively. The obtained parameter values are listed in Table 2 .

4 Applications of the inerter-based absorber

The proposed IBA involves connecting a reaction mass to the nacelle of the turbine at a single point via a combination of one inerter, one damper and two springs. In this paper, the initial condition is considered as the input for optimisation. Since the tower base bending moment is crucial to the tower fatigue life, the TTD is taken as the performance index, similar to [2]. Therefore, the objective function is defined as the standard deviation of the TTD:

$$J = std(\text{TTD}) \tag{7}$$

In order to identify the absorbers optimum layout and parameter values, objective function J is optimised using a combination of $patternsearch$ and $fminsearch$ in Matlab with $fminsearch$ refining the results obtained via $patternsearch$. The optimum configuration of the IBA is compared with the TMD to show its effectiveness.

Properties	Values
Hub mass	56,780 kg
Nacelle mass	240,000 kg
Rotor mass	110,000 kg
Tower mass	249,718 kg
Total turbine mass m_t	656,498 kg
Tower inertia I_t	2.73×10^9 kg·m^2
Platform mass m_p	7,466,330 kg
platform inertia I_p	5.01×10^{11} kg·m^2
Turbine's height to the tower hinge R	77.6 m
Turbine mass centre to the tower hinge R_t	64.5 m
Platform mass centre to the tower hinge R_t	-99.9155 m
Rotary stiffness of the tower k_t	1.56×10^{10} kN·m/rad
Rotary damping of the tower c_t	5.32×10^7 kN·m·s/rad
Rotary stiffness of the platform k_p	6.00×10^7 kN·m/rad
Rotary damping of the platform c_p	5.42×10^9 kN·m·s/rad

Table 2: Spar-buoy model parameters

4.1 Improvements with same absorber mass

In this section, the absorber's mass is taken to be 20000 kg for both TMD and IBA, with their optimum performances compared.

For the monopile case, the input load for optimisation procedure is an initial condition of TTD equal to 1 m. By using structure-immittance approach, the optimum IBA configuration and the corresponding parameter values are obtained. For the IBA case, the minimum value of the objective function is $J = 0.1782$ with $k_1 = 80.00$ kN/m, $k_2 = 7.21$ kN/m, $b = 1519$ kg, $c = 1.17$ kNs/m. For the TMD case, Y represents the velocity to force relation of a spring and a damper connected in parallel. The minimum value of the objective function is $J = 0.1909$ with $k = 82.60$ kN/m, $c = 8.393$ kNs/m. The performance improvement of the IBA is 6.65% compared with the TMD. Results are shown in Table 3 . The free decay responses of the monopile TTD with TMD and IBA in the nacelle are shown in Figure 5 .

Optimal parameter values and layouts	Vibration Absorber	
	TMD	2-springs IBA
J	0.1909	0.1782
Performance improvement	/	6.65%
Layouts	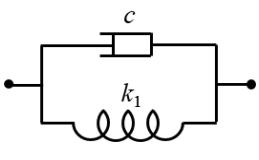	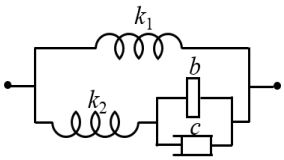
b	/	1519 kg
c	8.39 kNs/m	1.17 kNs/m
k_1	82.60 kN/m	80.00 kN/m
k_2	/	7.21 kN/m

Table 3: Optimisation results for monopile model

Similarly, for the spar-buoy case, the input load is an initial condition of tower TTD equal to 1 m. By using structure-immittance approach, the optimum IBA configuration and the corresponding parameter values are obtained. For the IBA case, the minimum value of the objective function is $J = 0.1667$ with $k_1 = 99.16$ kN/m, $k_2 = 9.26$ kN/m, $b = 1566$ kg, $c = 1.37$ kNs/m. The minimum value of the objective

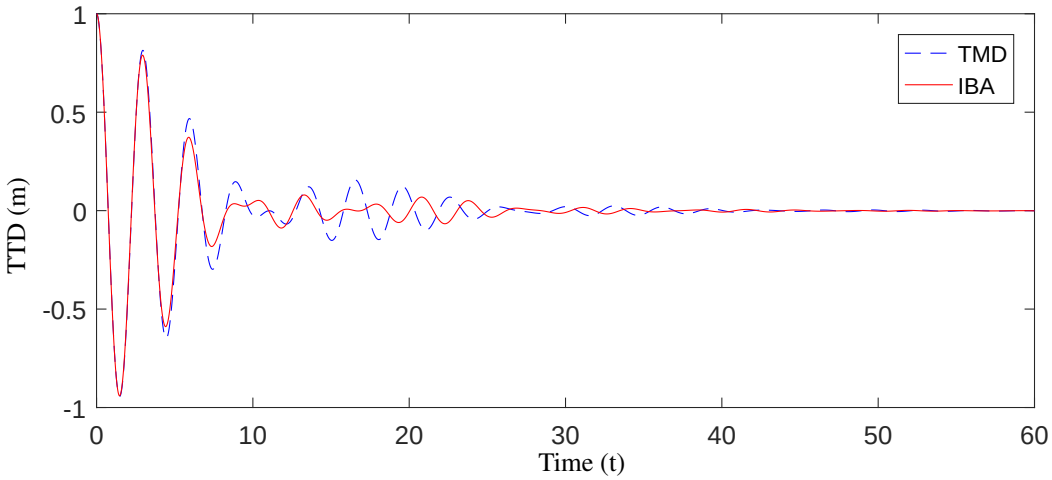

Figure 5: Free response of monopile TTD

function is $J = 0.1784$ with $k = 102.50$ kN/m, $c = 9.50$ kNs/m. The improvement of the IBVA is 6.56% compared with the TMD. The results are shown in Table 4. The free decay response of the spar-buoy tower top displacement and platform pitch angle with TMD and IBVA in the nacelle are shown in Figure 6 .

Optimal parameter values and layouts	Vibration Absorber	
	TMD	2-springs IBA
J	0.1784	0.1667
Performance improvement	/	6.56%
Layouts	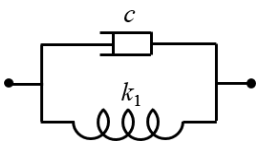	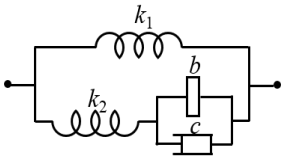
b	/	1566 kg
c	9.50 kNs/m	1.37 kNs/m
k_1	102.5 kN/m	99.16 kN/m
k_2	/	9.26 kN/m

Table 4: Optimisation results for spar-buoy model

4.2 Performances with different mass values

To assess the effect of mass on the optimum performance for TMD and IBA, mass values are taken as 10,000 kg, 20,000 kg and 40,000 kg, which are approximately 1%, 2% and 4% of the total mass of the monopile OWT. Using this information, compared with TMD of which mass value equals 20,000 kg, the possible mass reduction of the IBA while retaining the same level of performance is investigated.

For monopile, the input load for the optimisation procedure is the initial condition of TTD equal to 1 m. The monopile performance across a range of absorbers' mass values is shown in Figure 7 (a). It can be seen that as the mass value improves, the performance for both TMD and IBA are improved. However, the improvements of IBA is larger than that of the TMD. Moreover, compared to TMD with a 20,000 kg mass, the mass of IBA can be reduced to 16,785.7 kg (i.e. a 16.1% reduction) while achieving the same performance in terms of the cost function given in Eq. (7).

For spar-buoy, the input load for optimisation procedure is also the initial condition of TTD equal to 1 m. Relationships of the monopile performance with different absorbers' mass values is shown in Figure 7 (b).

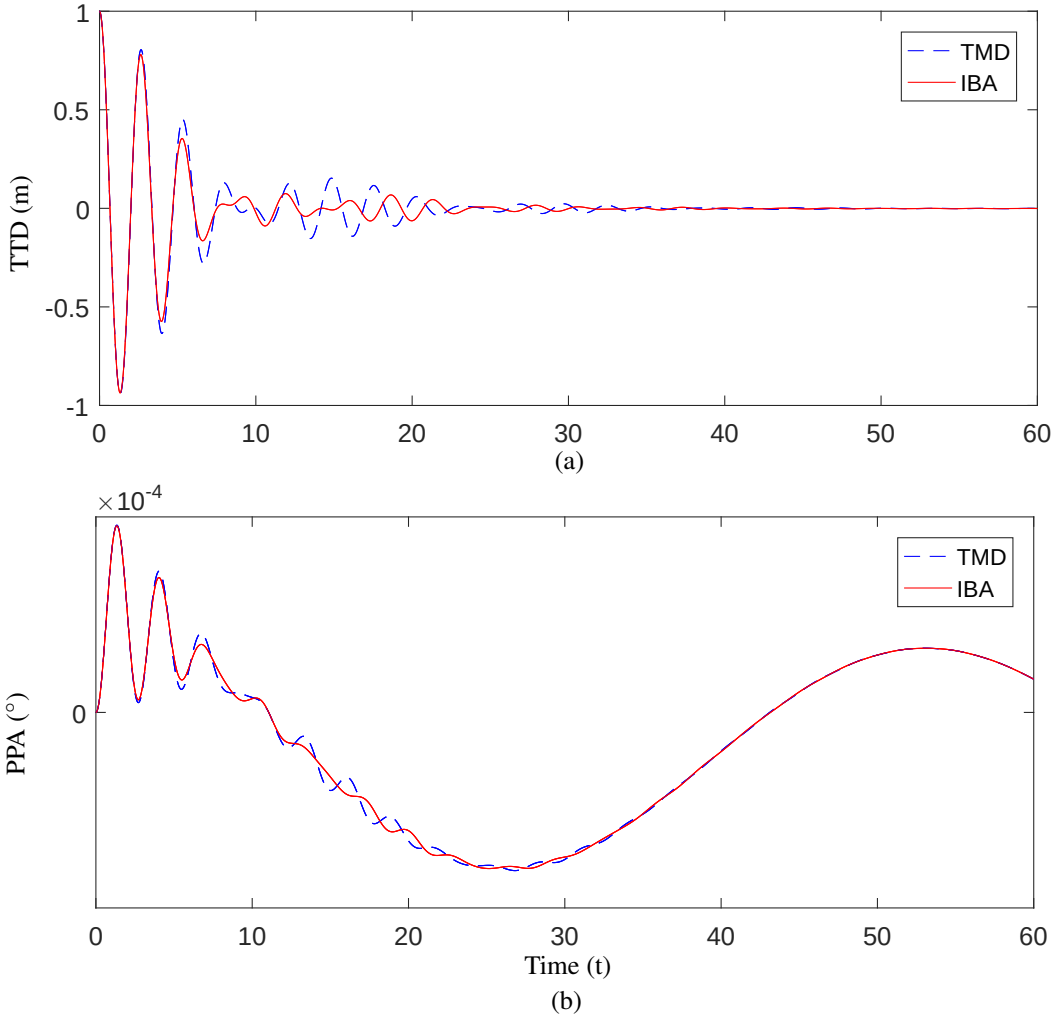

Figure 6: Free response of spar-buoy: (a) TTD; (b) PPA

Compared to TMD with a mass of 20,000 kg, the mass of IBA can be reduced to 14,996.9 kg (i.e. a 25.0% reduction) while achieving the same performance.

5 Conclusion and future work

In this paper, inerter-based absorbers are introduced in offshore wind turbine system to suppress its vibration. The absorber has a reaction mass connected to the nacelle at a single point using a combination of pre-determined number of inerters, dampers and springs. The concept of structure-immittance method is reviewed, which will facilitate the identification of the optimum absorber's layout and parameter values. The limited DOF Matlab models of monopile and spar-buoy are established, respectively, for the optimisation procedure. Since the tower bottom bending moment is the most fatigue loading, the standard deviation of tower top displacement is chosen as the reference index. The results show that the inerter-based absorber is superior to TMD in terms of reducing the tower top displacement. The reduction is 6.65% and 6.56% for monopile and spar-buoy, respectively, compared with TMD. Moreover, the relationship of performance with different mass values is also investigated. Compared with TMD, the mass can be reduced by 16.1% and 25.0% for monopile and spar-buoy, respectively, when employing an inerter-based device, while matching the performance of the TMD.

In our future work, the realistic wind and wave loads will be applied to the offshore wind turbine models in

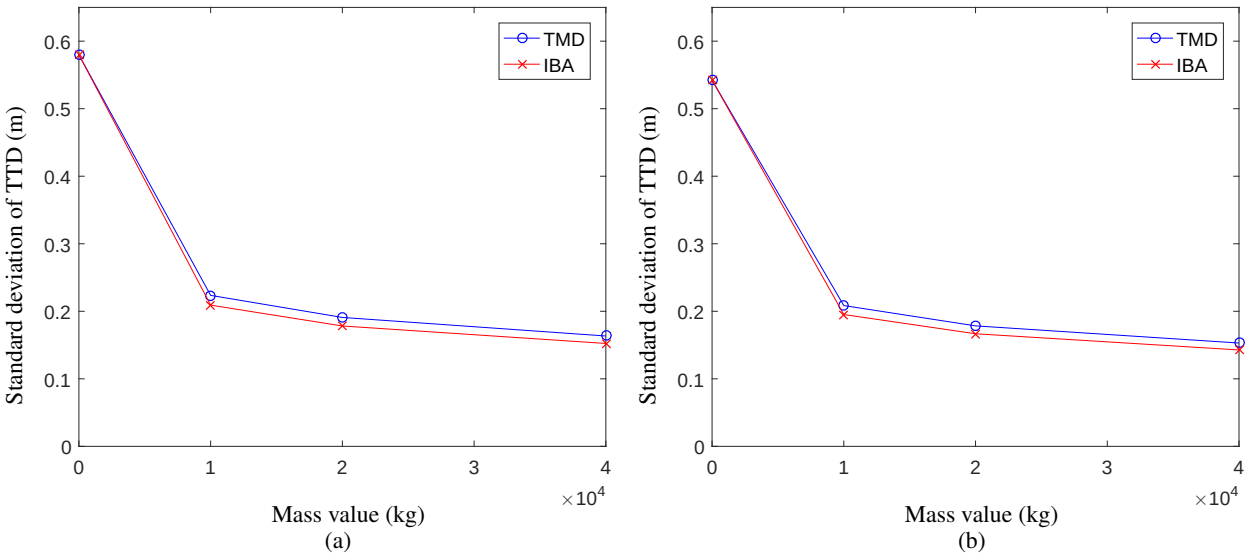

Figure 7: Performances for TMD and IBA with different mass values: (a) monopile; (b) spar-buoy

Matlab to further verify the efficiency of inerter-based absorbers in mitigating vibrations of turbines. Then the inerter and the structure-immittance method will be included in FAST for further optimisation to identify the most beneficial absorbers' layouts and their parameter values.

Acknowledgements

The authors would like to acknowledge the support of the University of Bristol, EPSRC and the Royal Society; Y-Y. L. is funded by the Deans Scholarship of Engineering Faculty; S. Y. Z. and J. Z. J are supported by the EPSRC grant EP/P013546/1; J. Z. J is also supported by a Royal Society project IE151194; S. A. N is supported by EPSRC fellowship EP/K005375/1.

References

[1] PJ. Murtagh, A. Ghosh, B. Basu, BM. Broderick, *Passive control of wind turbine vibrations including blade/tower interaction and rotationally sampled turbulence*, Wind Energy, Vol. 11, (2008), pp. 305-317.

[2] MA. Lackner, MA. Rotea, *Passive structural control of offshore wind turbines*, Wind Energy, Vol. 14, (2011), pp. 373-388.

[3] JM. Jonkman, ML. Buhl, *FAST User's Guide*, TP-500-38230, NERL, Golden, CO., (2011).

[4] G. Stewart, M. Lackner, *Offshore wind turbine load reduction employing optimal passive tuned mass damping systems*, IEEE Transactions on Control Systems Technology, Vol. 21, No.4, (2013), pp. 1090-1104.

[5] GM. Stewart, MA. Lackner, *The impact of passive tuned mass dampers and windwave misalignment on offshore wind turbine loads*, Engineering Structures, Vol. 73, (2014), pp. 54-61.

[6] Y. Si, HR. Karimi, H. Gao, *Modelling and optimization of a passive structural control design for a spar-type floating wind turbine*, Engineering Structures, Vol. 69, (2014), pp. 168-182.

[7] MC. Smith, *Synthesis of mechanical networks: the inerter*, IEEE Transactions on Automatic Control, Vol. 47, No. 10, (2002), pp. 1648-1662.

[8] FA. Firstone, *A new analogy between mechanical and electrical systems*, The Journal of the Acoustical Society of America, Vol. 4, No. 3, (1933), pp. 249-267.

[9] R. Bott, RJ. Duffin, *Impedance synthesis without use of transformers*, Journal of Applied Physics, Vol. 20, No. 8, (1949), pp. 816.

[10] IF. Lazar, SA. Neild, DJ Wagg, *Using an inerter-based device for structural vibration suppression*, Earthquake Engineering and Structural Dynamics, Vol. 43, No. 8, (2014), pp. 1129-1147.

[11] L. Marian, A. Giaralis, *Optimal design of a novel tuned mass-damper-inerter (TMDI) passive vibration control configuration for stochastically support-excited structural systems*, Probabilistic Engineering Mechanics, Vol. 38, (2014), pp. 156-164.

[12] FC. Wang, MR. Hsieh, HJ Chen, *Stability and performance analysis of a full-train system with inerters*, Vehicle System Dynamics, Vol. 50, (2012), pp. 545-571.

[13] Y. Li, JZ. Jiang, NA. Neild, *Inerter-based configurations for main-landing-gear shimmy suppression*, Journal of Aircraft, Vol. 54, (2014), pp. 684-693.

[14] SY. Zhang, JZ. Jiang, SA. Neild, *Passive vibration control: a structure-immittance approach*, Proceedings of the Royal Society, Vol. 473, (2017), 20170011.

[15] J. Jonkman, S. Butterfield, W. Musial, G. Scott, *Definition of a 5-MW reference wind turbine for offshore system development*, TP 500-38060, NREL, Golden, CO., (1997).

[16] J. Jonkman, S. Butterfield, P. Passon, T. Camp, J. Nichols, et al., *Offshore Code Comparison Collaboration within IEA Wind Annex XXIII: Phase II Results Regarding Monopile Foundation Modelling*, IEA European Offshore Wind Conference, Berlin, Germany, December 4-6, (2007).

[17] J. Jonkman, W. Musial, *Offshore code comparison collaboration (OC3) for IEA Task 23 offshore wind technology and deployment*, TP-5000-48191, NREL, Golden, CO., (2010).

[18] J. Jonkman, *Definition of the Floating System for Phase IV of OC3*, TP-500-47535, NREL, Golden, CO., (2010).